Enhanced Hydrolysis of Cellulose by Highly Dispersed Sulfonated Graphene Oxide

Lilan Huang, Hui Ye, Shaofei Wang, Yu Li, Yuzhong Zhang,* Weiguang Ma, Wenhan Yu, and Zhiyuan Zhou

Two-dimensional materials are promising for use as solid acids in cellulose hydrolysis. However, they suffer from a severe problem of restacking, which leads to poor solid-solid contact and decreased catalytic efficiency. Herein, highly dispersed sulfonated graphene oxide (GO-SO_3H) nanosheets were prepared and used as solid acids to hydrolyze cellulose. The highly dispersed GO-SO_3H was obtained by adding N,N-dimethylacetamide (DMAc). The DMAc improved the dispersibility of the GO-SO_3H nanosheets by increasing the zeta potential. The GO-SO_3H dispersion had the best dispersibility when the water/DMAc volume ratio was 1:10. The good dispersion of the catalysts increased the accessibility of acid sites to the β-1,4-glycosidic bonds in the cellulose, which led to a catalytic performance for hydrolyzing cellulose that was superior to that of any other system. When converting cellulose, the total reducing sugars and glucose yields were 78.3% and 69.7%, respectively, which were obtained within 8 h at 130 °C.

Keywords: Graphene oxide-based catalyst; Dispersibility; Reusability; Cellulose hydrolyzing

Contact information: State Key Laboratory of Separation Membranes and Membrane Processes, School of Materials Science and Engineering, Tianjin Polytechnic University, Tianjin 300387, China;
** Corresponding author: zhangyz2004cn@vip.163.com*

INTRODUCTION

With the progressive increase in global energy demands, the easily exploitable fossil fuel reserves will run out eventually. Moreover, extensive CO_2 emissions attributed to fossil fuel combustion have been associated with global climate change (Dutta 2012; Hu *et al.* 2015). To solve these problems, people must develop new environmentally friendly processes based on renewable feedstocks (Zhou *et al.* 2011). Cellulose biomass, the only sustainable source of organic carbon and the most abundant compound in the world, has been considered to be one of the most attractive candidates to replace fossil resources for the production of fuels, fuel additives, and fine chemicals (Dutta 2012; Wang *et al.* 2015).

Mineral acids, such as sulfuric acid, hydrochloric acid, and hydrofluoric acid, are efficient catalysts that have been widely used for converting cellulose to platform chemicals in various industries (Geboers *et al.* 2011). However, they suffer from problems, such as heavy reactor corrosion, difficult catalyst separation, and other environment-related issues (Nakajima and Hara 2012). Also, sulfuric acid readily degrades glucose at the high temperatures required for cellulose hydrolysis (Hu *et al.* 2014). A preference for a greener approach has stimulated the use of recyclable strong solid acids (Anastas and Kirchhoff 2002; Clark 2002). Among the various solid acids reported (Onda *et al.* 2008; Rinaldi *et al.* 2008; Lai *et al.* 2011), carbonaceous solid acid

was first reported by Hara *et al.* (2004) and has received considerable attention because of its unique structure and excellent catalytic performance. This solid acid is composed of uniformly functionalized graphene sheets with versatile groups, like -SO_3H, -COOH, and phenolic -OH. The strong Brønsted -SO_3H group as the catalytic site is linked to the rigid carbon skeleton directly, which leads to good stability. The -COOH and -OH groups can serve as polar adsorption sites to attract oxygen atoms from the β-1,4-glycosidic bonds in cellulose chains, and thus lead to superior catalytic activities (Suganuma *et al.* 2008; Kitano *et al.* 2009). Various carbonaceous solid acids have been prepared by the sulfonation of incompletely carbonized natural polymers, such as sugars and cellulose, and/or by incomplete carbonization of sulfopolycyclic aromatic compounds in concentrated sulfuric acid (Toda *et al.* 2005; Hara 2010; Fukuhara *et al.* 2011).

Among the carbon-based acid catalysts, graphene oxide (GO) is a promising candidate because of its layered quasi-homogenous structure and excellent thermal and water tolerances (Stankovich *et al.* 2006; Geim and Novoselov 2007). Its distinctive two-dimensional structure leads to a high degree of exposure of active sites on the surface, which enhances the accessibility of functional groups (Ji *et al.* 2011; Zhao *et al.* 2014). The new material not only has a similar catalytic mechanism with other bulky carbonaceous solid acids, but its high surface area can provide more catalytic sites, especially when GO is sulfonated. This makes sulfonated GO (sGO) more efficient for hydrolyzing cellulose. However, few studies have been conducted on hydrolyzing cellulose with sGO. Moreover, two-dimensional GO easily aggregates after sulfonation because of the high surface area and decreased charge. It can form irreversible agglomerates or even restack into three-dimensions in aqueous solutions in the absence of dispersing agents (Konkena and Vasudevan 2012; Park *et al.* 2016). This aggregation can decrease the availability of catalytic sites and overall efficiency. Wei *et al.* (2014) prepared sGO using chlorosulfonic acid, and the catalytic performance was investigated with cellobiose as the cellulose model. When cellobiose and sGO with a mass ratio of 1:10 were used, only 30.8% glucose was obtained. This may have been because of the low dispersion and bulky sGO that formed.

Researchers have made many efforts to improve the solid-solid contact between cellulose and catalysts. Yabushita *et al.* (2014) and Kobayashi *et al.* (2013) milled solid cellulose and solid catalyst together (mix-milling), which improved the conversion of cellulose. However, a long pretreatment time (24 h to 96 h) was needed to achieve the desired results, which is energy-intensive. It may be easier to enhance the solid-solid contact by improving the dispersion of solid catalyst in the reaction solutions (Jiang *et al.* 2010). As for GO, the dispersion is a colloidal system (Bourlinos *et al.* 2009; Behabtu *et al.* 2010) and the stability is mainly controlled by electrostatic repulsion between the charged colloidal particle surfaces. Therefore, the level of charging on it is the main concern (Everett 2007). The charge of GO sheets comes not only from the ionization of its own functional group, but also from electron transfer between GO sheets and solvent molecules (Jeong *et al.* 2008; Liu *et al.* 2012). According to the Lewis theory, the greater the electron donor number of an electron donor, the more negative the charge is on the electron acceptor (Lewis 1968; Gutmann 1978). Pure water cannot maintain the high dispersion of sGO. Thus, it is necessary to introduce a solvent with a higher electron donor number. At the same time, the solvent should facilitate the catalytic process through interaction with cellulose. For this, N,N-dimethylacetamide (DMAc) may be a good choice. Liu *et al.* (2012) reported that unfunctionalized graphene can be stable in DMAc because of its high electron donor number (27.8 kcal/mol) and low electron

acceptor number (13.6 kcal/mol). The zeta potential of the graphene/DMAc dispersion can reach -32 mV. Additionally, the solvent viscosity can influence the stability of colloidal systems. The viscosity of DMAc is 0.95 mPa·s, which is low and good for the dispersion of colloidal particles. More importantly, DMAc can cause intra- and inter-crystallite swelling and increase the accessibility of cellulose at high temperatures (Potthast *et al.* 2002; Klemm *et al.* 2004). Based on the previously mentioned studies, the dispersibility and stability of GO-based two-dimensional materials can be improved by adding solvents with high electron donor numbers.

In this work, sGO nanosheets were prepared by sulfonating GO with chlorosulfonic acid (GO-SO_3H) and then used as solid acids for hydrolyzing cellulose. The catalyst dispersibility was investigated by adding DMAc to water dispersions. The catalytic performance of the GO-SO_3H/water/DMAc system was investigated by hydrolyzing cellulose.

EXPERIMENTAL

Materials

The GO was synthesized in a strong oxidizing reaction with original graphite powder using the traditional Hummers method (Dimiev and Tour 2014). Graphite powder was obtained from Aladdin Chemical Reagent (Shanghai, China). Potassium permanganate ($KMnO_4$), concentrated sulfuric acid (H_2SO_4), sodium nitrate ($NaNO_3$), chlorosulfonic acid ($ClSO_3H$) (> 99.5%), and DMAc (99.5%) were purchased from Tianjin Guangfu Chemical Reagent (Tianjin, China). The CH_2Cl_2 was obtained from Kermel Chemical Reagent Corporation (Tianjin, China). Glucose (> 99.8%) and cellobiose (>99.5%) were obtained from Aladdin Chemical Reagent, along with α-cellulose (DP = 300). All of the chemicals were used without further purification. Deionized water was used throughout the whole experiment.

Methods

Catalyst preparation and characterization

The GO-SO_3H was synthesized from GO according to a method similar to that reported by Wei *et al.* (2014). Three grams of the obtained GO were dispersed in 300 mL of CH_2Cl_2 by sonication for 120 min. Subsequently, 30 mL of $ClSO_3H$ were added and the mixture was heated to 30 °C and stirred for 12 h. Finally, the mixture was repeatedly washed with deionized water by centrifugation until a neutral pH was obtained. After centrifugal washing, the product was freeze-dried to obtain the GO-SO_3H. Characterization of the catalysts was done with scanning electron microscopy (SEM) (S-4800, Hitachi, Tokyo, Japan), transmission electron microscopy (TEM) (H7650, Hitachi, Tokyo, Japan), Fourier transform infrared (FT-IR) spectroscopy (Nicolet iS50, Thermo Fisher, Waltham, USA), X-ray photoelectron spectroscopy (XPS) (K-Aepna, Thermo Fisher, Waltham, USA), X-ray diffraction (XRD) (D8 Discover, Bruker, Billerica, USA), Raman spectroscopy (XpoloRA PLUS, Horiba, Kyoto, Japan), and energy dispersive X-ray spectroscopy (EDS) (Octane Super, EDAX).

The density of the Brønsted acid sites (-SO_3H) in the GO-SO_3H was estimated by the sulfur content with elemental analysis (Vario EI cube, Elementar, Langenselbold, Germany). The total acid densities of the catalysts were determined by the acid-base titration method using NaCl (0.1 M) and NaOH solutions (0.01 M).

Catalyst dispersion in the solvents

A series of identical catalyst dispersions were prepared by dispersing the same amount of catalysts in mixed solvents with different water/DMAc ratios (v/v). These dispersions were sonicated at room temperature for 2 h.

To evaluate the dispersibility of the catalysts in the various mixed solvents, digital pictures of the standing dispersions with an irradiation of infrared light were captured by a digital camera (D750, Nikon corporation, Tokyo, Japan), and dispersion observations of the GO-SO_3H were performed using TEM. For further insight into the capability of the solvents to disperse catalysts, the zeta potential was determined with a zeta potential analyzer (Zetasizer Nano ZS90, Malvern, UK).

Catalyst reusability

The reusability of the GO-SO_3H was investigated *via* the hydrolysis reaction of water-soluble cellobiose with a cellobiose/catalyst ratio of 1:1 (wt/wt) at 130 °C for 8 h. The reaction was performed in a pressure kettle. The hydrolysate was centrifuged, and the catalyst was separated by decanting after the first cycle. Then, the supernatant was used to analyze the amount of glucose released and remaining cellobiose with a high-performance liquid chromatography (HPLC) system (Shimadzu LC-20 A, Shimadzu, Kyoto, Japan) consisting of an Agilent ZORBAX carbohydrate analysis column (250 mm × 4.6 mm) (Santa Clara, USA) and Shimadzu 20A refractive index detector (RID). The mobile phase consisted of acetonitrile and water at a ratio of 75:25 (v/v), and the flow rate was 1.5 mL/min. The separated GO-SO_3H was washed with deionized water several times and freeze-dried for the next reaction cycle.

Cellulose hydrolysis

Hydrolysis reactions were conducted in a 50-mL stainless-steel autoclave (YZHR-50, Shanghai Yanzheng Experimental Instrument Co. Ltd., Shanghai, China) with a Teflon insert. A certain amount of cellulose was added into each mixture containing a catalyst and the cellulose/catalyst ratio was 1:1. Then, the stainless-steel autoclave was heated at 130 °C for 8 h.

After the reaction, the catalyst was removed by centrifugation, and the supernatant was taken out with an injection syringe and filtered with a nylon syringe filter (0.45 μm). The analysis of the total reducing sugars (TRS) was conducted with the 3,5-dinitrosalicylic acid method (Miller 1959). The amount of produced glucose was analyzed by a HPLC system (Shimadzu, Kyoto, Japan) equipped with a carbohydrate analysis column (250 mm × 4.6 mm, Agilent) and RID (Shimadzu RID-20A) under the following conditions: a flow rate of 1.5 mL/min, mobile phase of acetonitrile/water (75:25, v/v), and column temperature of 30 °C. The product yield was expressed as the molar yield of the glucose and/or TRS products.

$$\textit{Yield of glucose}\ (\%) = \frac{glucose\ in\ hydrolysate\ (\mathrm{mol})}{anhydroglucose\ unit\ in\ cellobiose\ or\ cellulose\ (\mathrm{mol})} \times 100\% \qquad (1)$$

$$\textit{Yield of TRS}\ (\%) = \frac{glucose\ in\ reducing\ sugars\ (\mathrm{mol})}{anhydroglucose\ unit\ in\ cellulose\ (\mathrm{mol})} \times 100\% \qquad (2)$$

RESULTS AND DISCUSSION

Characterization

The surface morphology of the GO before and after sulfonation was studied using SEM. As a pretreatment, the samples were freeze-dried and then sputter coated with Au. The SEM images are shown in Fig. 1. It was clearly apparent from the SEM images that the GO-SO_3H had a similar structure to the GO. This unique structure of the catalyst has potential advantages in the acid-catalyzed hydrolysis reaction. First, the reactants could easily access the active sites on both sides of the two-dimensional graphene sheets. Second, the crumpling feature facilitates the diffusion of the product molecules (Ji *et al.* 2011; Wang *et al.* 2015). However, the increased crumples on the GO-SO_3H sheets revealed that the GO consisted of random aggregates after sulfonation and the crumpled sheets closely associated with each other, which formed agglomerate solids.

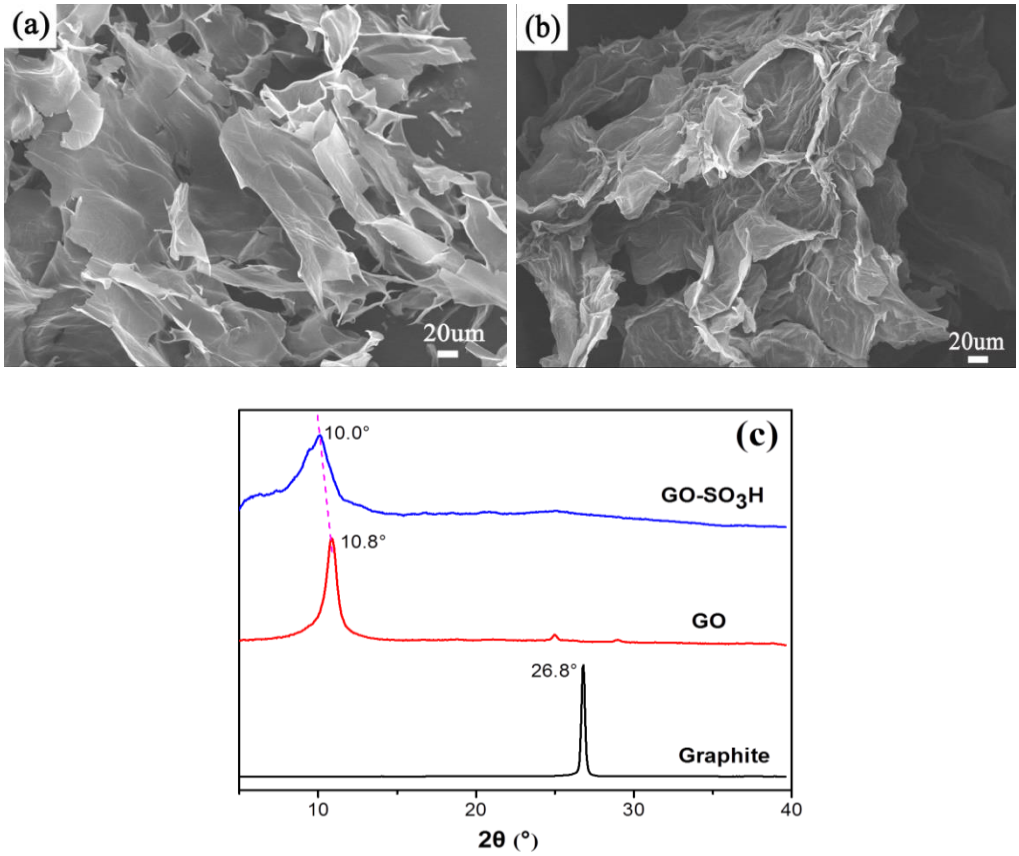

Fig. 1. SEM images of the GO (a) and GO-SO_3H (b); and XRD patterns (c)

The XRD analysis (Fig. 1c) showed that the 2θ degree peak of the pristine graphite was 26.8°, which suggested a well-known van der Waals thickness of 0.34 nm (Liu *et al.* 2008). After oxidation and exfoliation, the peak at a 2θ value of 26.8° completely disappeared and a new broader peak appeared at a 2θ value of 10.8°. The intercalating space of the GO sheets calculated according to the Bragg equation was 0.81 nm. When the GO was sulfonated, a broad main diffraction peak at 2θ equal to 10.0° was observed. The intercalating space of the GO-SO_3H increased to 0.9 nm, which indicated

that the new sulfonic acid groups (-SO_3H) were successfully attached to the GO sheets after sulfonation.

Additionally, the EDS mapping analysis (Fig. S2) of the GO-SO_3H revealed the homogenous distribution of sulfur elements over the entire range. The sulfur element mass percent in the GO (Fig. S1) was 2.22 wt.% (S = 0.69 mmol/g) according to the quantitative analysis, which was mainly generated in the preparation process. After sulfonation, the sulfur element mass percent of the GO-SO_3H was 3.24 wt.% (S = 1.02 mmol/g). This was ascribed to the formation of -SO_3H in the sulfonated reaction.

To demonstrate the formation of chemical bonding between the GO and sulfur, high-resolution XPS measurements were conducted (Fig. 2). In the wide scan (Fig. 2a), the peaks with binding energies of 531 eV, 286 eV, and 169 eV represented the adsorption peaks of O, C, and S, respectively. The data confirmed the presence of C, O, and S in the GO and GO-SO_3H. High-resolution C1s narrow spectra of the GO and GO-SO_3H were also scanned and are shown in Figs. 2b and 2c. The five peaks at 284.3 eV, 285.3 eV, 286.6 eV, 287.5 eV, and 289.1 eV corresponded to C-C/C-H, C-S, C-O, C=O, and C(=O)O bonds, respectively. These peaks represented -OH, -COOH, and -SO_3H groups. Additionally, the S2p core-level spectra only showed a single Gaussian distribution peak at 169.1 eV and this was ascribed to the bond energy site between -SO_3H and C. Thus, it was inferred that the sulfur in the catalyst, which possessed -COOH, -OH, and -SO_3H groups, was only contributed by the -SO_3H groups.

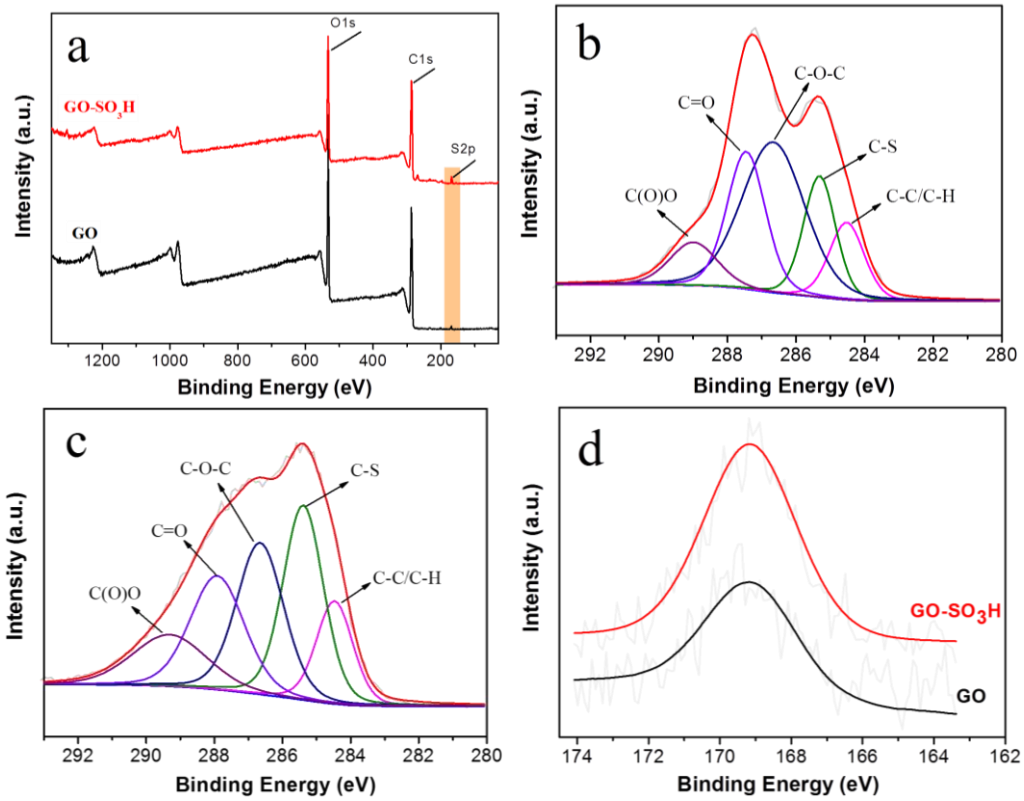

Fig. 2. XPS spectra of the GO and GO-SO_3H: wide scan (a); C1s core-level spectra of the GO (b) and GO-SO_3H (c); and S2p core-level spectra (d)

The density of the Brønsted acid sites (-SO_3H) in the GO-SO_3H was estimated by elemental analysis based on the sulfur content and was 1.05 mmol/g, which was similar

to the results obtained from the EDX mapping. Estimated by the acid-base titration method, the total acid density of the catalysts was 1.86 mmol/g. The phenolic -OH and -COOH in the catalyst would act as adsorption sites to adsorb and facilitate the hydrolysis of β-1,4-glycosidic bonds, which can improve the hydrolysis efficiency of the catalytic sites (-SO_3H) (Kitano *et al.* 2009). This was distinct from conventional solid acids with a single catalytic functional group.

Dispersion of the Catalyst

Cellulose is water-insoluble and possesses a robust crystal structure with a high chemical stability because of the strong inter- and intra-molecular hydrogen-bond network. Thus, for the hydrolysis of cellulose, the solid-solid contact between the solid acids and cellulose becomes a crucial factor in determining the efficiency of solid acid catalysts. The high dispersion of solid catalysts in the reaction solution could increase the accessibility of the active group on the catalysts to the reactive position in the cellulose. The density of the acid sites and acid strength are also important. The catalysts in this work had acid groups with appropriate densities of 1.86 mmol/g, so the focus was able to remain on improving the dispersion of catalysts in the reaction systems. As mentioned in the experimental section, the as-prepared GO-SO_3H was dispersed in water, DMAc, and water/DMAc mixtures with the aid of ultrasonication, and the dispersions were then allowed to settle for several weeks.

Figure 3 shows digital pictures of all of the dispersions after sonication for 2 h and after standing for a period of time after sonication. For the just sonicated dispersions, it was found that the GO-SO_3H powder showed a poor dispersibility in the water. The large undispersed catalyst particles were clearly seen on the side of the bottle. A semi-penetrating infrared beam caused by the Tyndall effect was also observed. For the DMAc and water/DMAc mixtures, the infrared beam was not observed, which indicated that the infrared light was adsorbed completely by the well-dispersed catalysts. It was still found that there were some fine particles on the bottle wall with the catalysts-DMAc dispersion. Logically, the catalyst-water dispersion showed a short-term stability and precipitated after 12 h. The catalyst-DMAc dispersion did not show obvious stratification and precipitates because of the darker color of the dispersion, but a short infrared beam was also observed after 12 h, which indicated that the stability of this dispersion was not as good. The infrared light path was still not observed for the catalyst-water/DMAc dispersion even after 9 weeks, which suggested that the GO-SO_3H had a strong stability in the water/DMAc mixture with a ratio of 1:10 (v/v).

It was further seen from the TEM images (Fig. S3) that the GO-SO_3H was difficult to disperse in water. The catalyst particles showed poor transmittance on the micro grid copper network because of the aggregation of undispersed GO-SO_3H layers. When the GO-SO_3H was dispersed in DMAc, the transmittance of the particles was improved, which indicated good dispersion of the GO-SO_3H sheets. The crimples on the GO-SO_3H were more obvious with more DMAc in the solvent mixture. The GO-SO_3H layers were still not single-layer in the water/DMAc mixture (1:10 v/v), which suggested that the catalyst was dispersed incompletely because of the effect of drying and the sulfonation process. It was still found that the GO-SO_3H layers showed better transmittance and that most of them were dispersed uniformly in the solvent.

The dispersion/aggregation state of the GO-SO_3H sheets in the solvents was monitored by measuring their zeta potential to gain further insight into the colloidal

stability. The zeta potentials of the GO-SO_3H dispersed in various solvents are shown in Fig. 4.

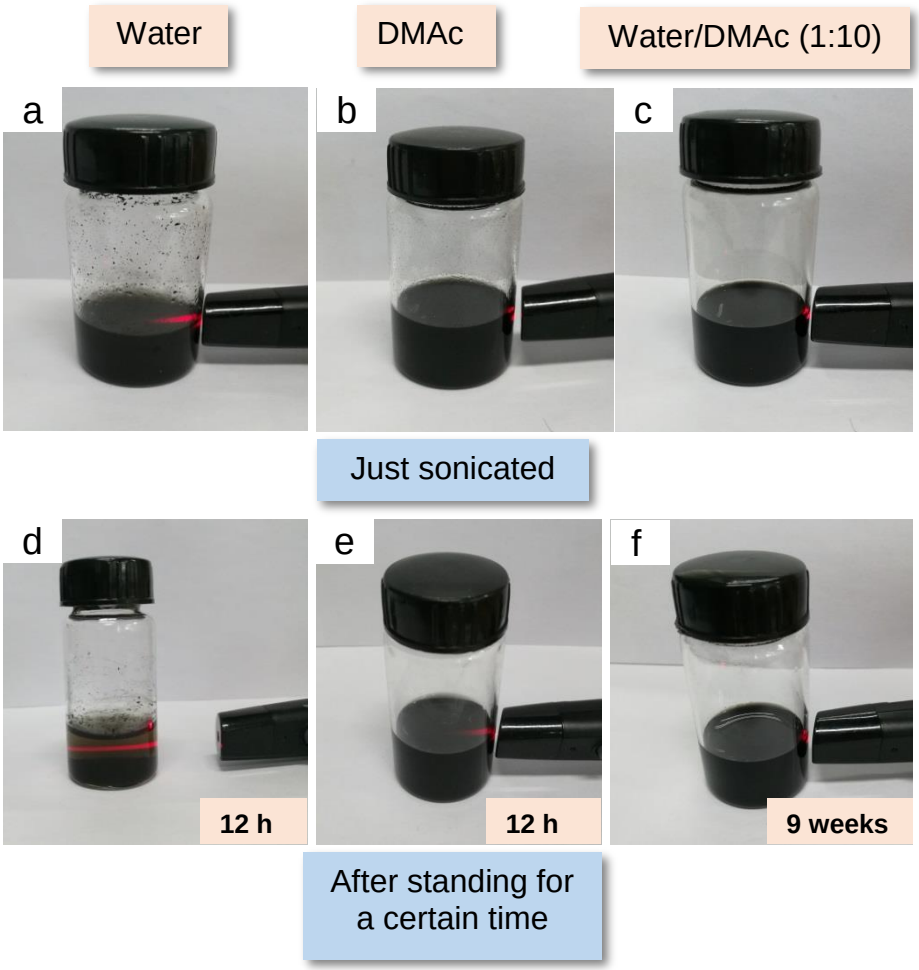

Fig. 3. Digital pictures of the as-prepared GO-SO_3H dispersed in different solvents with ultrasonic-assisted for 2 h: dispersions immediately after sonication (a, b, and c); dispersions 12 h with the water system (d), 12 h with the DMAc system (e), and 9 weeks with the water/DMAc system after sonication (f)

All of the dispersions were negatively charged. The zeta potential of the GO dispersed in water was -45.23 mV because of the ionization of the abundant oxygen-containing functional group. After sulfonation, the GO-SO_3H dispersed in water was less charged, and the zeta potential was -28.75 mV because of the partial elimination of -OH and -COOH groups. The zeta potential of the GO-SO_3H in pure DMAc was -30.52 mV, which indicated that GO-SO_3H in DMAc was more charged than in water. This was because DMAc has a higher electron donor number. Additionally, the zeta potential further increased when the catalyst was dispersed in the water/DMAc mixture because of both ionization and electron transfer. The electrostatic repulsion between the charged GO-SO_3H sheet surfaces led to a stable dispersion. Zeta potential values beyond the -30 mV to +30 mV region are considered to represent sufficient mutual repulsion to ensure the stability of a dispersion, as is well known from colloidal science (Everett 2007). The dispersions of the GO-SO_3H in this study were near this range. When using the

water/DMAc (1:10 v/v) mixture as the solvent, the zeta potential even reached -45 mV, which indicated good dispersibility and stability.

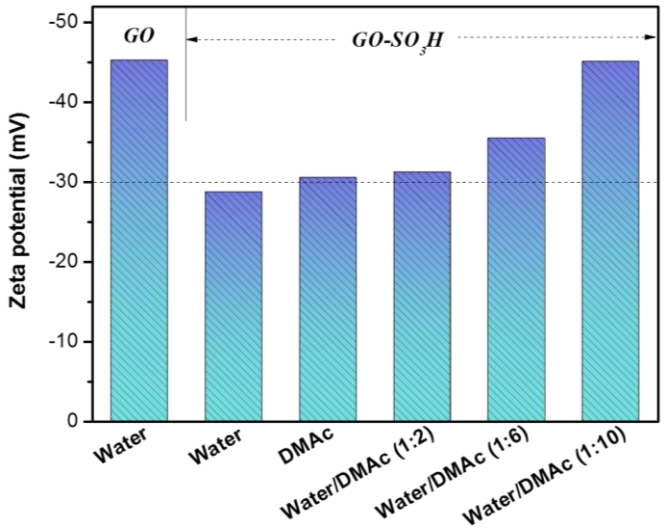

Fig. 4. Zeta potentials of the GO and GO-SO_3H suspensions

Catalyst Stability

To investigate the stability of the catalysts, sequential hydrolytic reactions were conducted with cellobiose (50 mg) as the substrate at 130 °C for 8 h per cycle. Initially, preliminary degradation of the glucose measurement at different temperatures was performed to confirm the appropriate reaction temperature. The reaction temperature had a remarkable influence on the degradation of glucose (Fig. S4). After reacting for 8 h, the degradation of glucose reached 15.5%, 20.0%, 48.0%, and 63.8% at the reaction temperatures of 80 °C, 130 °C, 150 °C, and 180 °C, respectively. Higher temperatures led to faster degradation of the glucose. However, the cellulose was unstable and more likely to degrade when the temperature was higher than 120 °C. Taking this into consideration, the reaction temperature of 130 °C was chosen for the subsequent hydrolysis experiments.

Figure 5 shows the stability of the GO-SO_3H solid acid by measuring the released glucose and cellobiose conversion in different cycles. The catalyst retained 92.4% of its original relative activity after five cycles (Fig. 5b). Reusability is a main advantage of solid catalysts because it can reduce pollution and lower operation costs (Guo *et al.* 2012). The catalyst used in this study showed a good stability.

The loss of efficiency in the repeating process might have been because of the high temperature and large amount of water, which led to leaching of the -SO_3H groups. In this process, the cellobiose conversion and glucose yield decreased from 85.0% to 78.1% and from 82.4% to 76.2%, respectively (Fig. 5a). This is ascribed to the leaching of –SO_3H in reaction and the detail is listed in Table 1. However, no remarkable difference was observed between the cellobiose conversion and glucose yield over the entire process, which indicated that glucose was not further decomposed into byproducts, such as 5-hydroxymethylfurfural, formic acid, and organic acids. The results also supported recent research that found cellobiose adsorbed on the GO sheets would occupy the active catalytic sites until the cellobiose was hydrolyzed completely (Zhao *et al.* 2014). Thus, the glucose would not be degraded until the total conversion of cellobiose was achieved. The glucose selectivity was stable at 97.6%.

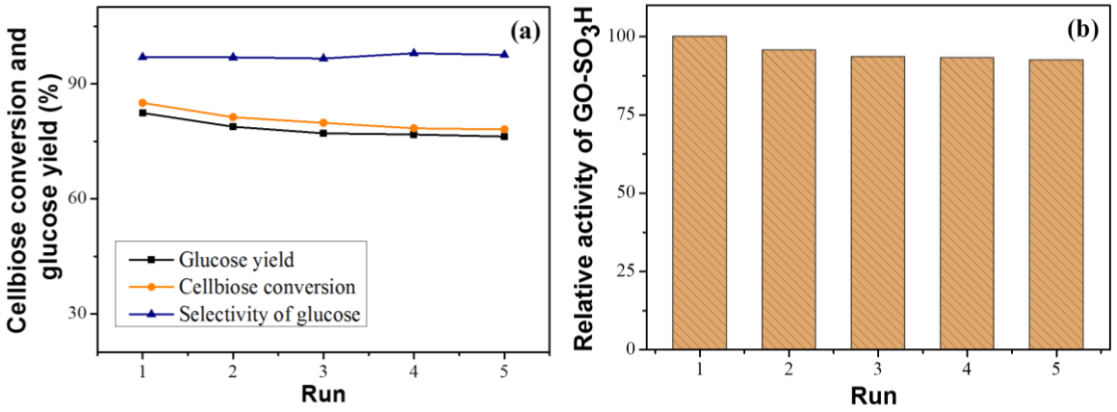

Fig. 5. Hydrolysis of the cellobiose by GO-SO_3H (a) and relative activity of the GO-SO_3H (b) over five cycles

Table 1. The Density of Acidic Groups in Used Catalysts

Runs	Run 1	Run 2	Run 3	Run 4	Run 5
Density of –SO_3H in used catalysts (mmol/g)	1.05	0.87	0.81	0.77	0.68

A FT-IR analysis was performed to gain further insight into the stability of catalysts through changes in their structure (Fig. 6a). The -OH stretching at 3441 cm^{-1} and C=O stretching in -COOH groups at 1720 cm^{-1} were observed in the GO and GO-SO_3H. Compared with the GO, the GO-SO_3H exhibited a stronger band at 1051 cm^{-1} corresponding to -SO_3 symmetric stretching (Ludvigsson *et al.* 2000; Hu *et al.* 2007) and a new peak at 877 cm^{-1} corresponding to S-OH stretching, which indicated the successful grafting of -SO_3H groups onto the GO sheets. When the catalyst was reused five times, the characteristic peak of -SO_3H at 1051 cm^{-1} was reduced.

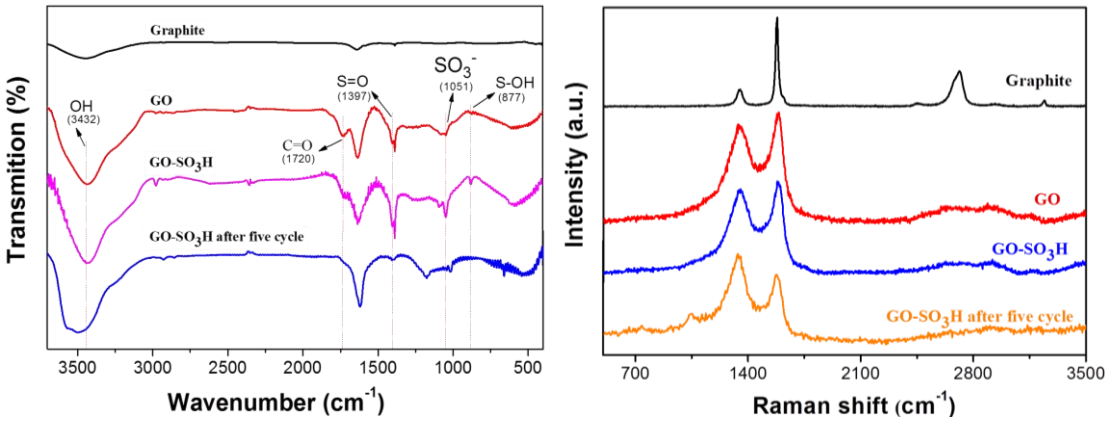

Fig. 6. FT-IR (a) and Raman (b) spectra of the graphite GO, fresh GO-SO_3H, and GO-SO_3H after five reaction cycles

Structural changes were also reflected in the Raman spectra (Fig. 6b). The Raman spectrum of the pristine graphite displayed a prominent G peak at 1581 cm^{-1}, which corresponded to the first-order scattering of the E2g mode (Tuinstra and Koenig 1970). In

the Raman spectra of the GO and GO-SO_3H, the G band broadened and shifted to 1587 cm^{-1}. Moreover, the D band located at 1345 cm^{-1} became prominent, which indicated a reduction in the size of the in-plane sp^2 domains. This was possibly because of the extensive oxidation and sulfonation. The Raman spectrum also contained both G (1580 cm^{-1}) and D bands (1331 cm^{-1}) when the GO-SO_3H was recycled five times, along with an increased D/G intensity ratio. This change suggested a decrease in the average size of the sp^2 domains upon reduction of the catalyst at high reaction temperatures and new graphitic domains were created (Tuinstra and Koenig 1970). It was suggested that although the catalyst was stable, there were still some -SO_3H groups that leached during the reusable process because of the high temperature and high proportion of water.

Hydrolysis of the Cellulose

To confirm the effect of catalyst dispersion on the catalytic performance, catalyzed hydrolysis of the cellulose was performed. The amount of catalyst in all of the dispersions was 50 mg. An equal mass of cellulose was added. The results are summarized in Table 2. The catalyst dispersed in DMAc (Entry 2) could not hydrolyze the cellulose because of the absence of H_2O and subsequent H_3O^+, which is essential for cleavage of glycosidic bonds (Shafie *et al.* 2014). Entry 4 to Entry 6 show that the water/DMAc/catalyst systems had better catalytic performances than the water system (Entry 3). The water/catalyst system yielded only 0.8% TRS and no glucose. The TRS yield increased from 1.7% to 52.4% when the water/DMAc (v/v) ratio decreased from 1:2 to 1:10. In the case of the 1:10 ratio, the glucose yield was 45.1% and the glucose selectivity reached 86.1%. To identify the different contributions of the Brønsted acid concentration and dispersion, a contrast test was performed and is listed as Entry 1. The amount of water used in Entry 1 was equal to that in Entry 5, but no DMAc was used. With this condition, the amount of H_3O^+ was consistent for Entry 1 and Entry 5. However, the TRS yield of Entry 1 was lower than that of Entry 5. This indicated that the dispersion of GO-SO_3H had a more pronounced effect on the catalytic performance when cellulose was used as the substrate material.

The catalytic property of the GO-SO_3H with different dispersibility was also evaluated by testing the hydrolysis of amorphous cellulose. The results are shown in Table 2. In this study, α-cellulose was pretreated with phosphoric acid and ball-milling to obtain amorphous cellulose. From the XRD analysis (Fig. S5), it was seen that amorphous cellulose had a notably lower crystallinity, so it was more accessible by solid acid compared with the non-pretreated microcrystalline cellulose. The molar yields of TRS and glucose from the two types of amorphous cellulose (Entry 9 and Entry 13) were greater than that from the non-pretreated cellulose (Entry 6) at the same reaction conditions. Amorphous cellulose-1 (pretreated by phosphoric acid) was more likely to be degraded than amorphous cellulose-2 (pretreated by ball-milling) because of the lower crystallinity, and the TRS and glucose yields reached 78.3% and 69.7%, respectively, after an 8-h reaction (Entry 9). The TRS and glucose yields from amorphous cellulose-1 and amorphous cellulose-2 increased with an increased reaction time (Entry 7 to Entry 9 and Entry 11 to Entry 13, respectively). However, a longer reaction time (24 h) led to a lower TRS yield because further degradation might have occurred (Entry 10 and Entry 14). In any case, the glucose selectivity maintained a high level (85.3% to 90.5%) for hydrolyzing either pretreated or non-pretreated cellulose by GO-SO_3H dispersed in water/DMAc (1:10 v/v). The leaching of –SO_3H took place in each reaction, and the detail is listed in Table 3.

In addition, the contribution of the solubilization of cellulose by DMAc was also investigated. Heated reactions were performed at 130°C of α-cellulose in aqueous dilute sulfuric acid mixtures both with DMAc as a co-solvent and without DMAc at 0.1 M acid concentration and measured the percent solubilization of the α-cellulose. The results revealed that the presence of DMAc as a water-miscible co-solvent enhanced the solubilization of cellulose in comparison to the water-only solvent system and further improved by increasing DMAc (Fig. 7.), which demonstrate the advantage of DMAc-water co-solvent. The high dispersion of GO-SO_3H nanosheets and the enhanced solubilization of α-cellulose caused by the addition of DMAc led to the effective cellulose conversion.

Table 2. Hydrolysis of the Cellulose by GO-SO_3H

Entry	Substrate	Dispersion Water/DMAc (v/v)	Reaction Time (h)	TRS (%)	Glucose (%)
1	Avicel cellulose	4.3 mL of water, no DMAc[a]	8	2.7	1.4
2	Avicel cellulose	0/1	8	-	-
3	Avicel cellulose	1/0	8	0.8	-
4	Avicel cellulose	1/2	8	1.7	0.4
5	Avicel cellulose	1/6	8	13.8	8.6
6	Avicel cellulose	1/10	8	52.4	45.1
7	Amorphous cellulose-1[b]	1/10	3	36.3	30.9
8	Amorphous cellulose-1	1/10	5	65.8	55.1
9	Amorphous cellulose-1	1/10	8	78.3	69.7
10	Amorphous cellulose-1	1/10	24	22.8	19.5
11	Amorphous cellulose-2[c]	1/10	3	32.4	27.9
12	Amorphous cellulose-2	1/10	5	50.1	43.4
13	Amorphous cellulose-2	1/10	8	71.2	64.4
14	Amorphous cellulose-2	1/10	24	23.7	20.3

Reaction conditions: catalysts = 50 mg, cellulose = 50 mg, reaction temperature = 130 °C, and volume of the reaction solution = 30 mL; [a] the amount of water was equal to the amount of water used in Entry 5, but no DMAc was used; [b] Amorphous cellulose-1: cellulose pretreated by phosphoric acid and regenerated; [c] Amorphous cellulose-2: cellulose pretreated by ball-milling for 20 h.

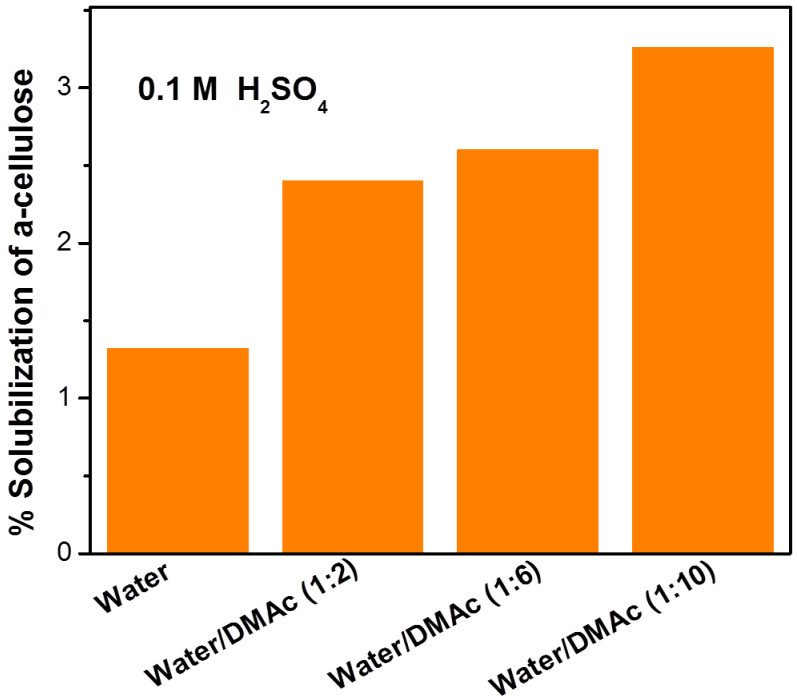

Fig. 7. Comparison of the % solubilization of α-cellulose in heated bath reaction solvated in water-only or in DMAc-water co-solvent mixtures at 0.1 M dilute sulfuric acid concentration. The reaction temperature was 130 °C and the duration was 2 h for all reactions.

Table 3. The Density of Acidic Groups in Used Catalysts After 8h Reaction

Water/DMAc (v/v)	1:2	1:6	1:10
Density of $-SO_3H$ in used catalysts (mmol/g)	0.76	0.84	0.88

Comparison with Other Carbon-based Solid Acids

To obtain an overview of the catalytic performance of carbon-based solid acid in different solvents for cellulose hydrolysis, a comparison was made, and the results are shown in Table 4. The GO-SO_3H dispersed in water/DMAc with a ratio of 1:10 exhibited a higher TRS yield and glucose selectivity than the other catalyst dispersions. It was inferred that the high conversion of resistant cellulose could be achieved by improving the dispersibility of the carbonaceous solid acid.

Table 4. Comparison of the Catalytic Performance with Other Carbonaceous Solid Acids

Catalyst	Substrate	Catalyst/ Sub-strate (wt/wt)	Total Acid Densities (mmol/g)	T (°C)	Time (h)	TRS (%)	Glucose (%)	Ref.
$CH_{0.62}O_{0.54}S_{0.05}$	Avicel cellulose	12:1	1.9	130	3	64	4	(Suganuma *et al.* 2008)
SUCRA-SO_3H	Avicel cellulose	2:1	0.28	120	24	48	4	(Hu *et al.* 2014)
SUCRO-SO_3H	Avicel cellulose	2:1	0.47	120	24	26	3	
Glycerol based solid acid	Amorphous cellulose	1:1	-	160	4	19.4	-	(Goswami *et al.* 2015)
$Si_{66}C_{33}$-823-SO_3H	Amorphous cellulose	1:1	0.15	150	24	36	38	(Van de Vyver *et al.* 2010)
PRCSA	Amorphous cellulose	2:1	1.8	-	-	39	34	(Shen *et al.* 2013)
Fe_3O_4-RGO-SO_3H	Avicel cellulose	1:1	1.56	150	3	-	28	(Yang *et al.* 2015)
sGO	Cellobiose	10:1	2.2	120	8	40.5	37.2	(Wei *et al.* 2014)
GO-SO_3H	Cellobiose	1:1	1.86	130	8	85	82.4	This work
GO	Avicel cellulose	1:1	0.88	130	8	15.6	8.7	This work
GO-SO_3H	Avicel cellulose	1:1	1.86	130	8	52.4	45.1	This work
GO-SO_3H	Amorphous cellulose-2	1:1	1.86	130	8	71.2	64.4	This work
GO-SO_3H	Amorphous cellulose-1	1:1	1.86	130	8	78.3	69.7	This work

CONCLUSIONS

1. The catalyst dispersion with a water/N,N-dimethylacetamide (DMAc) ratio of 1:10 was more effective for cellulose hydrolysis than the other carbonaceous solid acids under similar reaction conditions. This has provided a new approach for the hydrolysis of cellulose in heterogeneous catalytic systems.
2. The total reducing sugars (TRS) yield was increased by increasing the dispersibility of the catalysts because the accessibility of acid sites to the β-1,4-glycosidic bonds in the cellulose was improved. The catalyst dispersion with a water/DMAc ratio of 1:10 converted the microcrystalline cellulose into TRS and glucose with yields of 52.4% and 45.1%, respectively. When amorphous cellulose was introduced, 78.3% TRS and 69.7% glucose were obtained at the same reaction conditions.

3. The addition of DMAc into water not only improved the dispersibility of the sulfonated graphene oxide (GO-SO_3H) nanosheets by increasing the zeta potential, but it also enhanced the solubilization of cellulose to some extent. These made the cellulose conversions are more effective.

ACKNOWLEDGMENTS

The authors are grateful for the support of the National Natural Science Foundation of China (Grants No. 51373120, 51503146, and 21676201).

REFERENCES CITED

Anastas, P. T., and Kirchhoff, M. M. (2002). "Origins, current status, and future challenges of green chemistry," *Accounts Chem. Res.* 35(9), 686-694. DOI: 10.1021/ar010065m

Behabtu, N., Lomeda, J. R., Green, M. J., Higginbotham, A. L., Sinitskii, A., Kosynkin, D. V., Tsentalovich, D., Parra-Vasquez, A. N., Schmidt, J., Kesselman, E., *et al*. (2010). "Spontaneous high-concentration dispersions and liquid crystals of graphene," *Nat. Nanotechnol.* 5(6), 406-411. DOI: 10.1038/nnano.2010.86

Bourlinos, A. B., Georgakilas, V., Zboril, R., Steriotis, T. A., and Stubos, A. K. (2009). "Liquid-phase exfoliation of graphite towards solubilized graphenes," *Small* 5(16), 1841-1845. DOI: 10.1002/smll.200900242

Clark, J. H. (2002). "Solid acids for green chemistry," *Accounts Chem. Res.* 35(9), 791-797. DOI: 10.1021/ar010072a

Dimiev, A. M., and Tour, J. M. (2014). "Mechanism of graphene oxide formation," *ACS Nano* 8(3), 3060-3068. DOI: 10.1021/nn500606a

Dutta, S. (2012). "Catalytic materials that improve selectivity of biomass conversions," *RSC Adv.* 2(33), 12575-12593. DOI: 10.1039/c2ra20922e

Everett, D. H. (2007). *Basic Principles of Colloid Science*, Royal Society of Chemistry, London, UK.

Fukuhara, K., Nakajima, K., Kitano, M., Kato, H., Hayashi, S., and Hara, M. (2011). "Structure and catalysis of cellulose-derived amorphous carbon bearing SO_3H groups," *ChemSusChem* 4(6), 778-784. DOI: 10.1002/cssc.201000431

Geboers, J. A., Van de Vyver, S., Ooms, R., Op de Beeck, B., Jacobs, P. A., and Sels, B. F. (2011). "Chemocatalytic conversion of cellulose: Opportunities, advances and pitfalls," *Catal. Sci. Technol.* 1(5), 714-726. DOI: 10.1039/C1CY00093D

Geim, A. K., and Novoselov, K. S. (2007). "The rise of graphene," *Nat. Mater.* 6(3), 183-191. DOI: 10.1038/nmat1849

Goswami, M., Meena, S., Navatha, S., Rani, K. N. P., Pandey, A., Sukumaran, R. K., Prasad, R. B. N., and Devi, B. L. A. P. (2015). "Hydrolysis of biomass using a reusable solid carbon acid catalyst and fermentation of the catalytic hydrolysate to ethanol," *Bioresour. Technol.* 188, 99-102. DOI: 10.1016/j.biortech.2015.03.012

Guo, F., Fang, Z., Xu, C. C., and Smith Jr., R. L. (2012). "Solid acid mediated hydrolysis of biomass for producing biofuels," *Prog. Energ. Combust.* 38(5), 672-690. DOI: 10.1016/j.pecs.2012.04.001

Gutmann, V. (1978). *The Donor-acceptor Approach to Molecular Interactions*, Springer US, New York City, NY.

Hara, M. (2010). "Biomass conversion by a solid acid catalyst," *Energ. Environ. Sci.* 3(5), 601-607. DOI: 10.1039/B922917E

Hara, M., Yoshida, T., Takagaki, A., Takata, T., Kondo, J. N., Hayashi, S., and Domen, K. (2004). "A carbon material as a strong protonic acid," *Angew. Chem. Int. Edit.* 116(22), 3015-3018. DOI: 10.1002/ange.200453947

Hu, J., Baglio, V., Tricoli, V., Aricò, A. S., and Antonucci, V. (2007). "PEO-PPO-PEO triblock copolymer/Nafion blend as membrane material for intermediate temperature DMFCs," *J. Appl. Electrochem.* 38(4), 543-550. DOI: 10.1007/s10800-007-9471-5

Hu, L., Lin, L., Wu, Z., Zhou, S., and Liu, S. (2015). "Chemocatalytic hydrolysis of cellulose into glucose over solid acid catalysts," *Appl. Catal. B–Environ.* 174-175, 225-243. DOI: 10.1016/j.apcatb.2015.03.003

Hu, S., Smith, T. J., Lou, W., and Zong, M. (2014). "Efficient hydrolysis of cellulose over a novel sucralose-derived solid acid with cellulose-binding and catalytic sites," *J. Agr. Food Chem.* 62(8), 1905-1911. DOI: 10.1021/jf405712b

Jeong, H.-K., Yun, P. L., Lahaye, R. J. W. E., Park, M.-H., An, K. H., Kim, I. J., Yang, C.-W., Park, C. Y., Ruoff, R. S., and Lee, Y. H. (2008). "Evidence of graphitic AB stacking order of graphite oxides," *J. Am. Chem. Soc.* 130(4), 1362-1366. DOI: 10.1021/ja076473o

Ji, J., Zhang, G., Chen, H., Wang, S., Zhang, G., Zhang, F., and Fan, X. (2011). "Sulfonated graphene as water-tolerant solid acid catalyst," *Chem. Sci.* 2(3), 484-487. DOI: 10.1039/C0SC00484G

Jiang, Y., Li, X., Cao, Q., and Mu, X. (2010). "Acid functionalized, highly dispersed carbonaceous spheres: An effective solid acid for hydrolysis of polysaccharides," *J. Nanopart. Res.* 13(2), 463-469. DOI: 10.1007/s11051-010-0153-6

Kitano, M., Yamaguchi, D., Suganuma, S., Nakajima, K., Kato, H., Hayashi, S., and Hara, M. (2009). "Adsorption-enhanced hydrolysis of β-1,4-glucan on graphene-based amorphous carbon bearing SO_3H, COOH, and OH groups," *Langmuir* 25(9), 5068-5075. DOI: 10.1021/la8040506

Klemm, D., Philipp, B., Heinze, T., Heinze, U., and Wagenknecht, W. (2004). "General considerations on structure and reactivity of cellulose," in: *Comprehensive Cellulose Chemistry: Fundamentals and Analytical Methods, Volume 1*, Wiley-VCH Verlag, Weinheim, Germany.

Kobayashi, H., Yabushita, M., Komanoya, T., Hara, K., Fujita, I., and Fukuoka, A. (2013). "High-yielding one-pot synthesis of glucose from cellulose using simple activated carbons and trace hydrochloric acid," *ACS Catal.* 3(4), 581-587. DOI: 10.1021/cs300845f

Konkena, B., and Vasudevan, S. (2012). "Understanding aqueous dispersibility of graphene oxide and reduced graphene oxide through pK_a measurements," *J. Phys. Chem. Lett.* 3(7), 867-872. DOI: 10.1021/jz300236w

Lai, D.-m., Deng, L., Guo, Q.-x., and Fu, Y. (2011). "Hydrolysis of biomass by magnetic solid acid," *Energ. Environ. Sci.* 4(9), 3552-3557. DOI: 10.1039/C1EE01526E

Lewis, G. N. (1968). *Valence and the Structure of Atoms and Molecules*, Dover Publications, New York City, NY.

Liu, N., Luo, F., Wu, H., Liu, Y., Zhang, C., and Chen, J. (2008). "One-step ionic-liquid-assisted electrochemical synthesis of ionic-liquid-functionalized graphene sheets directly from graphite," *Adv. Funct. Mater.* 18(10), 1518-1525.

DOI: 10.1002/adfm.200700797
Liu, W. W., Wang, J. N., and Wang, X. X. (2012). "Charging of unfunctionalized graphene in organic solvents," *Nanoscale* 4(2), 425-428. DOI: 10.1039/C1NR10921A
Ludvigsson, M., Lindgren, J., and Tegenfeldt, J. (2000). "FTIR study of water in cast Nafion films," *Electrochim. Acta* 45(14), 2267-2271. DOI: 10.1016/S0013-4686(99)00438-7
Miller, G. L. (1959). "Use of dinitrosalicylic acid reagent for determination of reducing sugar," *Anal. Chem.* 31(3), 426-428. DOI: 10.1021/ac60147a030
Nakajima, K., and Hara, M. (2012). "Amorphous carbon with SO_3H groups as a solid Brønsted acid catalyst," *ACS Catal.* 2(7), 1296-1304. DOI: 10.1021/cs300103k
Onda, A., Ochi, T., and Yanagisawa, K. (2008). "Selective hydrolysis of cellulose into glucose over solid acid catalysts," *Green Chem.* 10(10), 1033-1037. DOI: 10.1039/B808471H
Park, M., Song, K., Lee, T., Cha, J., Lyo, I., and Kim, B.-S. (2016). "Tailoring graphene nanosheets for highly improved dispersion stability and quantitative assessment in nonaqueous solvent," *ACS Appl. Mater. Inter.* 8(33), 21595-21602. DOI: 10.1021/acsami.6b07272
Potthast, A., Rosenau, T., Sixta, H., and Kosma, P. (2002). "Degradation of cellulosic materials by heating in DMAc/LiCl," *Tetrahedron Lett.* 43(43), 7757-7759. DOI: 10.1016/S0040-4039(02)01767-7
Rinaldi, R., Palkovits, R., and Schüth, F. (2008). "Depolymerization of cellulose using solid catalysts in ionic liquids," *Angew Chem. Int. Edit.* 47(42), 8047-8050. DOI: 10.1002/anie.200802879
Shafie, Z. M., Yu, Y., and Wu, H. (2014). "Insights into the primary decomposition mechanism of cellobiose under hydrothermal conditions," *Ind. Eng. Chem. Res.* 53(38), 14607-14616. DOI: 10.1021/ie5027309
Shen, S., Wang, C., Cai, B., Li, H., Han, Y., Wang, T., and Qin, H. (2013). "Heterogeneous hydrolysis of cellulose into glucose over phenolic residue-derived solid acid," *Fuel* 113, 644-649. DOI: 10.1016/j.fuel.2013.06.021
Stankovich, S., Dikin, D. A., Dommett, G. H. B., Kohlhaas, K. M., Zimney, E. J., Stach, E. A., Piner, R. D., Nguyen, S. T., and Ruoff, R. S. (2006). "Graphene-based composite materials," *Nature* 442(7100), 282-286. DOI: 10.1038/nature04969
Suganuma, S., Nakajima, K., Kitano, M., Yamaguchi, D., Kato, H., Hayashi, S., and Hara, M. (2008). "Hydrolysis of cellulose by amorphous carbon bearing SO_3H, COOH, and OH groups," *J. Am. Chem. Soc.* 130(38), 12787-12793. DOI: 10.1021/ja803983h
Toda, M., Takagaki, A., Okamura, M., Kondo, J. N., Hayashi, S., Domen, K., and Hara, M. (2005). "Green chemistry: Biodiesel made with sugar catalyst," *Nature* 438(7065), 178. DOI: 10.1038/438178a
Tuinstra, F., and Koenig, J. L. (1970). "Raman spectrum of graphite," *J. Chem. Phys.* 53(3), 1126-1130. DOI: 10.1063/1.1674108
Van de Vyver, S., Peng, L., Geboers, J., Schepers, H., de Clippel, F., Gommes, C. J., Goderis, B., Jacobs, P. A., and Sels, B. F. (2010). "Sulfonated silica/carbon nanocomposites as novel catalysts for hydrolysis of cellulose to glucose," *Green Chem.* 12(9), 1560-1563. DOI: 10.1039/C0GC00235F
Wang, J., Xi, J., and Wang, Y. (2015). "Recent advances in the catalytic production of glucose from lignocellulosic biomass," *Green Chem.* 17(2), 737-751. DOI: 10.1039/C4GC02034K

Wei, Z., Yang, Y., Hou, Y., Liu, Y., He, X., and Deng, S. (2014). "A new approach towards acid catalysts with high reactivity based on graphene nanosheets," *ChemCatChem* 6(8), 2354-2363. DOI: 10.1002/cctc.201402100

Yabushita, M., Kobayashi, H., Hara, K., and Fukuoka, A. (2014). "Quantitative evaluation of ball-milling effects on the hydrolysis of cellulose catalysed by activated carbon," *Catal. Sci. Technol.* 4(8), 2312-2317. DOI: 10.1039/C4CY00175C

Yang, Z., Huang, R., Qi, W., Tong, L., Su, R., and He, Z. (2015). "Hydrolysis of cellulose by sulfonated magnetic reduced graphene oxide," *Chem. Eng. J.* 280, 90-98. DOI: 10.1016/j.cej.2015.05.091

Zhao, X., Wang, J., Chen, C., Huang, Y., Wang, A., and Zhang, T. (2014). "Graphene oxide for cellulose hydrolysis: How it works as a highly active catalyst?," *Chem. Commun.* 50(26), 3439-3442. DOI: 10.1039/C3CC49634A

Zhou, C.-H., Xia, X., Lin, C.-X., Tong, D.-S., and Beltramini, J. (2011). "Catalytic conversion of lignocellulosic biomass to fine chemicals and fuels," *Chem. Soc. Rev.* 40(11), 5588-5617. DOI: 10.1039/C1CS15124J

Article submitted: July 30, 2018; Peer review completed: September 29, 2018; Revised version received and accepted: October 16, 2018; Published: October 22, 2018.
DOI: 10.15376/biores.13.4.8853-8870